

## Magnetism and spin-polarized transport in carbon atomic wires

Z. Y. Li,<sup>1</sup> W. Sheng,<sup>1</sup> Z. Y. Ning,<sup>2</sup> Z. H. Zhang,<sup>3</sup> Z. Q. Yang,<sup>1,\*</sup> and H. Guo<sup>2</sup>

<sup>1</sup>Surface Physics Laboratory (National Key Laboratory), Fudan University, Shanghai 200433, China

<sup>2</sup>Center for the Physics of Materials and Department of Physics, McGill University, Montreal, Quebec, Canada H3A 2T8

<sup>3</sup>School of Physics and Electronic Science, Changsha University of Science and Technology, Changsha 410076, China

(Received 5 May 2009; revised manuscript received 19 July 2009; published 24 September 2009)

We report *ab initio* calculations of magnetic and spin-polarized quantum transport properties of pure and nitrogen-doped carbon atomic wires. For finite-sized wires with even number of carbon atoms, total magnetic moment of  $2\mu_B$  is found. On the other hand, wires with odd number atoms have no net magnetic moment. Doped with one or two nitrogen atom(s), the carbon atomic wires exhibit a spin-density-wave-like state. The magnetic properties can be rationalized through bonding patterns and unpaired states. When the wire is sandwiched between Au electrodes to form a transport junction, perfect spin filtering effect can be induced by slightly straining the wire.

DOI: 10.1103/PhysRevB.80.115429

PACS number(s): 73.22.-f, 71.15.Nc, 85.65.+h

Due to the remarkably long spin coherence time, magnetism, and quantum transport in carbon nanostructures have attracted considerable attention for possible applications in spintronics.<sup>1</sup> Spin polarization in carbon structures may come from proximity to ferromagnetic metal<sup>2,3</sup> or from doped transition metal atoms such as Fe, Cr, or V, etc.<sup>4-6</sup> Carbon-based systems such as exohedral or endohedral fullerenes [ $C_{60}N$  (Ref. 7) and  $N@C_{60}$  (Ref. 8), etc.] were also found to have local magnetic moments and these fullerene systems are considered useful for quantum information technology.<sup>8</sup> Very interestingly, even pure carbon structure is predicted to have magnetism such as that occurring along the zigzag edges<sup>9,10</sup> of graphene nanoribbons, or near vacancies<sup>11</sup> in graphene. The theoretical prediction and successful experimental fabrication of single-layer graphene<sup>12</sup> have triggered substantial interests in exploiting magnetism in pure carbon systems. Magnetism found in materials containing only *s* and *p* electrons, instead of traditionally localized *d* or *f* electrons, should be extremely interesting to spintronics.

Magnetism occurring in carbon nanostructures is usually rather localized, e.g., magnetic edge states along the boundary of zigzag graphene nanoribbons<sup>9,10</sup> or magnetic moments due to dangling bonds and vacancies.<sup>11</sup> In general, the origin of magnetism in pure carbon nanostructures has not been understood to high satisfaction. In particular, when carbon nanostructures are contacted by nonmagnetic metal electrodes to form a transport device, an important question is how magnetic character of the carbon system is influenced by the electrodes. This issue is of fundamental importance if magnetism in pure carbon nanostructure is to be exploited for spintronics application. It is the purpose of this paper to report our investigation on this issue.

To be specific, we focus on magnetism and spin-polarized quantum transport in carbon atomic wires which are important for molecular-scale electronics due to their stable and extremely thin structures.<sup>5,6,13-20</sup> By using chemical techniques, linear carbon atomic wires containing up to 20 atoms has been synthesized experimentally.<sup>21,22</sup> A number of interesting charge transport properties have been predicted for carbon atomic wires sandwiched between two metal leads, including even-odd oscillatory conductance,<sup>13</sup> negative dif-

ferential resistance,<sup>14</sup> and distinct stretching features.<sup>14-16</sup> Magnetoresistance effect was also predicted when transition metal atoms were doped in the wires.<sup>6,18-20</sup> Magnetism and transport in pure or *sp*-element-doped carbon wires, however, have not been reported so far.

Here we investigate magnetic properties of pure and nitrogen-doped carbon atomic wires using *ab initio* methods. For finite length wires having an even number of carbon atoms, a total magnetic moment of  $2\mu_B$  was found where the magnetism is mostly localized at the ends of the wires. No magnetism is found for the odd-numbered carbon wires. When doped with one or two nitrogen atom(s), the wire exhibits a spin-density-wave-like (SDW-like) state indicating a “long range” magnetism, namely the magnetism is not just localized at the ends of wire. All the magnetic properties can be well understood through bonding patterns and unpaired states that exist in the wires. When these atomic wires are contacted by metal leads to form two-probe transport junctions, the leads are found to severely diminish the magnetism. Almost perfect spin filtering effect by the carbon atomic wire, however, can be restored by slightly straining the wire and this effect is true even for intrinsically nonmagnetic wires. These results strongly suggest that transport junctions formed by short carbon atomic wires have extremely interesting magnetic properties that can be exploited for spin-polarized quantum transport.

We investigate magnetic properties of short carbon atomic wires shown in Fig. 1(a) using *ab initio* plane-wave density-functional theory (DFT) calculations.<sup>23</sup> The pseudopotentials generated with projector-augmented wave method at the level of generalized-gradient approximation (GGA) were employed.<sup>24</sup> The energy cutoff is set to be 350 eV. The interatomic distances in all the wires were obtained by relaxing the structures until the Hellmann-Feynman forces were less than 0.01 eV/Å. For quantum transport, we use a state-of-the-art first-principles technique where real space DFT is carried out within the Keldysh nonequilibrium Green’s function (NEGF) formalism.<sup>25</sup> The basic idea of the NEGF-DFT formalism is to calculate device Hamiltonian and electronic structure by DFT, deal with the nonequilibrium quantum transport conditions by NEGF, and account for the open device boundary conditions by real space numerical procedure.

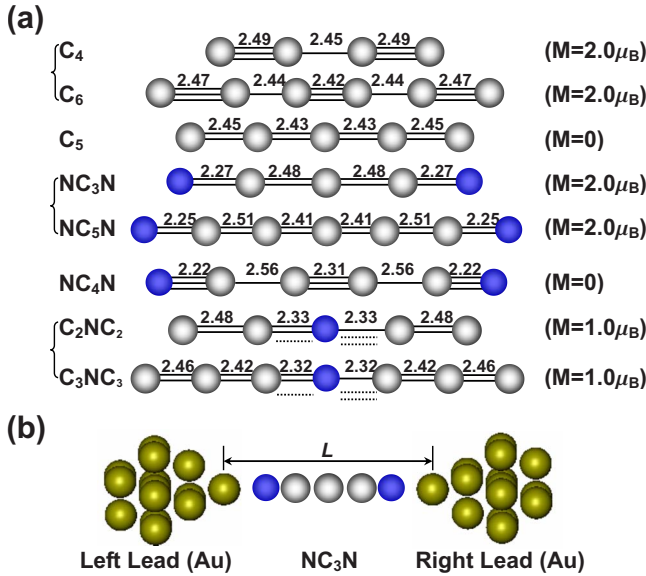


FIG. 1. (Color online) (a) Several typical atomic wires studied. The optimized bond lengths (in a.u.), the obtained total magnetic moment (M), and the bonding patterns formed are given for each wire. (b) A schematic of the transport device, where an atomic wire of NC<sub>3</sub>N is sandwiched as an example between two Au electrodes.

After the self-consistent NEGF-DFT iteration of the charge density is converged to  $1.0^{-4}$ , we calculate transmission coefficients and spin-polarized currents from standard Green's function method.<sup>25</sup> We refer interested readers to Ref. 25 for details of the NEGF-DFT formalism. The geometry of the transport device is indicated in Fig. 1(b), where an atomic wire of NC<sub>3</sub>N is sandwiched as an example between two gold electrodes extending to  $z = \pm \infty$  (transport direction). The Au electrodes are oriented along the (111) direction with finite cross section.<sup>26</sup> Four layers of each electrode in the contacts are considered as buffer layers. The local geometries of the contacts for the leads are assumed to be cone-like<sup>27</sup> to mimic an scanning tunnel microscope (STM) tip. The bulk bond length (5.44 a.u.) is chosen for Au-Au distance in the leads. At equilibrium, the distance between the two protruding gold atoms of electrodes ( $L_0$ ) is obtained by relaxing Au-NC<sub>3</sub>N-Au wire. Similar processes were conducted for other atomic wires. For the case of NC<sub>3</sub>N wire, the calculated equilibrium distance  $L_0 = 16.82$  a.u. and the bond length of Au-N is 3.69 a.u. For transport calculations, we also present a small degree of strain to the atomic wire by fixing the distance between the two protruding gold atoms to certain value ( $L = L_0 + \Delta L$ ) and the atoms between the two gold atoms are relaxed to find their optimal positions.

Several kinds of short atomic wires are investigated including pure carbon wires with even number of carbon atoms (C<sub>2n</sub>, where n is an integer), odd-numbered pure carbon wires (C<sub>2n+1</sub>), carbon wires terminated with two nitrogen atoms (NC<sub>2n</sub>N and NC<sub>2n+1</sub>N), and even-numbered carbon wires doped with one nitrogen atom at the center (C<sub>n</sub>NC<sub>n</sub>). Except for C<sub>2n+1</sub> and NC<sub>2n</sub>N, the C<sub>2n</sub>, NC<sub>2n+1</sub>N, and C<sub>n</sub>NC<sub>n</sub> wires show magnetism with total magnetic moments of  $2\mu_B$ ,  $2\mu_B$ , and  $1\mu_B$ , respectively, as indicated in Fig. 1(a). These values of the total magnetic moment do not change with

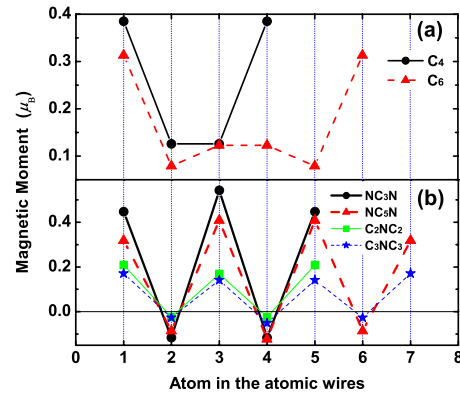


FIG. 2. (Color online) Local magnetic moment on each atom in (a) the even-numbered carbon wires (C<sub>4</sub> and C<sub>6</sub>) and (b) the nitrogen-doped wires (NC<sub>3</sub>N and NC<sub>5</sub>N; C<sub>2</sub>NC<sub>2</sub> and C<sub>3</sub>NC<sub>3</sub>).

respect to the number of carbon atoms in each type of wires. Thus, each type of atomic wires has a similar magnetic behavior. For the three types of magnetic carbon wires, we found the energy differences between the magnetic ground states and nonmagnetic states are all around 0.1 eV, i.e., significantly larger than  $k_B T$  of room temperature. It suggests that pure carbon atomic wires in the nanoscale can have non-trivial magnetism even in normal conditions. Local magnetic moment on each atom in the magnetic wires is given in Fig. 2. For even-numbered carbon wires, the magnetic moments are mainly localized at the two terminal atoms; while for other two kinds of magnetic wires (NC<sub>2n+1</sub>N and C<sub>n</sub>NC<sub>n</sub>), interesting SDW-like states appear. Therefore, for even-numbered carbon wires, only localized magnetism at the ends is found. But for carbon wires doped with one or two nitrogen atoms, the magnetism distributes in the whole wire, indicating a long range magnetism (albeit for the short wire).

The different magnetic behavior for different types of wires can be understood by analyzing bonding patterns in the wire. For each atomic wire, the optimized interatomic distances were given in Fig. 1(a). Calculations of structural relaxation indicate that the C-C bond lengths near the wire ends tend to elongate slightly, consistent with the trend obtained by Senapati *et al.*<sup>20</sup> After considering the boundary effect, the bonding pattern in even-numbered carbon atomic wires can be qualitatively assigned to alternating  $\sigma$  and multiple  $\pi$  bonds in the ground states [see C<sub>4</sub> and C<sub>6</sub> in Fig. 1(a)]. For the odd-numbered wires, the bonding pattern is a  $\pi$ -conjugated structure [see C<sub>5</sub> in Fig. 1(a)]. For C<sub>2n</sub>, the  $\sigma$ - $\pi$  bonding pattern leads to the two terminal atoms unsaturated with unpaired states. These two unpaired states give rise to the  $2\mu_B$  total magnetic moment in the wires. Since the  $\sigma$  bonds can act as tunnel barriers,<sup>20</sup> the magnetism mostly localizes at the terminals as shown in Fig. 2(a). On the other hand, for C<sub>2n+1</sub>, the  $\pi$ - $\pi$  conjugated bonding pattern does not leave unpaired states at the terminals, hence no magnetism in the wires. Therefore, it is the bonding pattern and unpaired states that determine whether or not a carbon wire has magnetism. This picture should be helpful in understanding magnetism for other pure carbon nanostructures.<sup>9-11</sup>

The bonding patterns of the N-doped wires of NC<sub>2n+1</sub>N and NC<sub>2n</sub>N are the same as those of C<sub>2n+1</sub> and C<sub>2n</sub>, respec-

tively. The magnetic structures of the N-doped wires are, however, different. The bonding pattern in the  $\text{NC}_{2n+1}\text{N}$  wires causes one unpaired state at each terminal, acquiring  $2\mu_B$  magnetic moment. All the saturated bonds in the  $\text{NC}_{2n}\text{N}$  wires mean nonmagnetism for these wires. The magnetic behavior of  $\text{NC}_n\text{N}$  is somewhat different from the case of carbon atomic wires terminated with three-dimensional transition metal (TM) atoms.<sup>6</sup> As shown in Ref. 6, the magnetic structure of the two end TM atoms usually oscillates between parallel and antiparallel arrangements, depending on whether there is an even or odd number of carbon atoms separating the moments. The difference can be ascribed to the distinct origins of the magnetism in our system and theirs. For  $\text{NC}_n\text{N}$  wires, it is the unpaired  $p$  states that produce the magnetism and both N and C atoms tend to form saturated bonds with the neighbors to form stable structure. These characteristics lead to no magnetism in  $\text{NC}_{2n}\text{N}$  wires. Due to structural symmetry, a twofold degenerate bonding patterns exists around the N atom in  $\text{C}_n\text{NC}_n$ , expressed by the solid and dotted lines in Fig. 1(a). The dopant N induces one unpaired state in the wire leading to  $1\mu_B$  total magnetic moment. Since  $\pi$ - $\pi$  conjugated bonding pattern can enhance interference of states at different atoms, this bonding pattern makes the magnetic structure of  $\text{NC}_{2n+1}\text{N}$  and  $\text{C}_n\text{NC}_n$  SDW-like, such that magnetism is now distributed in the entire wire. This long range magnetism is very different from that of the  $\text{C}_{2n}$  wires where magnetic moments are mainly localized at the terminals.

When the carbon wire is contacted by Au electrodes to form a two-probe transport junction [see Fig. 1(b)], magnetism is found to be severely diminished by the metal electrodes: this is true even for  $\text{NC}_{2n+1}\text{N}$  and  $\text{C}_n\text{NC}_n$  wires which, when free standing, have nonlocalized magnetic distribution as discussed above. The reason can be ascribed to the disappearance of unpaired states in the wires because of the electrodes. A spin-polarized current, however, can still be induced by stretching slightly the wires. This process can be accomplished in STM experiments by moving the STM tip to elongate the atomic wire.<sup>28</sup> Figure 3 plots transmission coefficients of the two-probe atomic wires with certain stretching  $\Delta L$ . The wires in Figs. 3(a)–3(c) have intrinsic magnetism, while those in Figs. 3(d) and 3(e) have not. Surprisingly, our results show that spin-polarized current can be induced in all the wires with or without intrinsic magnetism by stretching. The features of spin-dependent transport are, however, different for the two kinds of wires. For wires with intrinsic magnetism, it is the minority states that mainly contribute to conduction as seen from Figs. 3(a)–3(c). Especially, near 100% spin-polarized current can be obtained in the case of  $\text{NC}_3\text{N}$  and  $\text{C}_2\text{NC}_2$ . The efficiency of this spin filtering effect is comparable with or even higher than that from magnetic contacts or organometallic samples.<sup>18,29</sup> The spin polarization in the intrinsically nonmagnetic  $\text{C}_5$  and  $\text{NC}_4\text{N}$  devices is found to be induced by gold atoms of the electrodes near the carbon wires. For the  $\text{C}_5$  and  $\text{NC}_4\text{N}$  devices, it is the majority states that conduct, contrary to that of  $\text{NC}_3\text{N}$ ,  $\text{C}_2\text{NC}_2$ , and  $\text{C}_4$  devices as will be explained below. The transmission coefficients with different stretching length are also calculated. As shown in Fig. 3(a), the spin resonant peak near the Fermi level ( $E_F$ ) becomes sharper and moves a little to lower energies with increase in the stretching. The

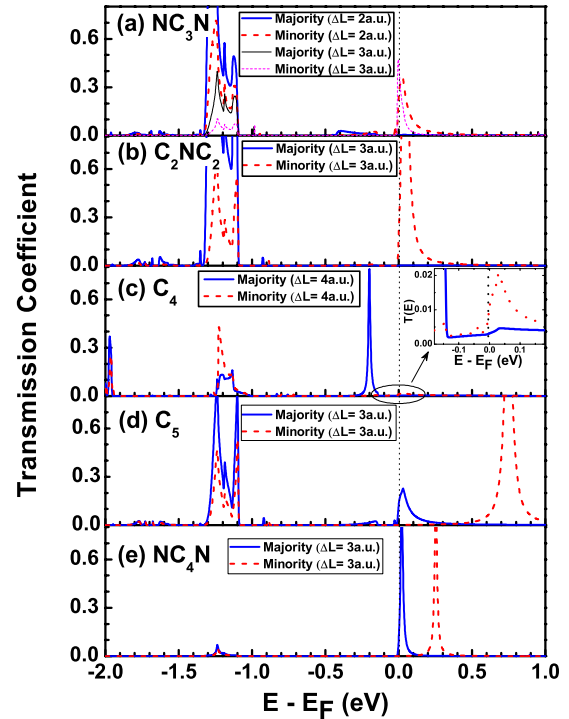


FIG. 3. (Color online) Transmission coefficient versus energy for different typical wires: (a)  $\text{NC}_3\text{N}$ , (b)  $\text{C}_2\text{NC}_2$ , (c)  $\text{C}_4$ , (d)  $\text{C}_5$ , and (e)  $\text{NC}_4\text{N}$ . The majority and minority express the different spin directions.  $\Delta L$  gives the stretching length between two Au electrodes. The inset in (c) shows the transmission coefficient near the Fermi level ( $E_F$ ).

spin filtering effect consequently becomes more profound with a little longer stretching length. For N-doped wires [Figs. 3(a), 3(b), and 3(e)], there are usually high transmission peaks located near  $E_F$ , indicating good conducting characteristic induced by the dopant N.

To further understand the role of nitrogen-doping and spin-dependent transport, the density of states (DOS) of typical wires are calculated. Figures 4(a)–4(c) shows the DOS of the  $\text{NC}_3\text{N}$ ,  $\text{C}_4$ , and  $\text{NC}_4\text{N}$  devices, respectively. Note that the DOS coming from buffer layers of Au leads are eliminated in these figures. Very obvious spin splitting can be seen from the DOS, especially for  $\text{NC}_3\text{N}$  wire. Due to strong affinity of N atoms, some of the occupied states move to lower energy after the N atoms are doped. From the analysis of partial DOS (not shown), it is known that the transmission peaks near  $E_F$  in N-doped wires are mainly induced by N ( $2p$ ) states, although C ( $2s$  and  $2p$ ) also contributes significantly. This explains why the N-doped wires have higher transmission than that of pure carbon wires. Figure 4 also indicates that minority states are located near  $E_F$  in the  $\text{NC}_3\text{N}$  and  $\text{C}_4$  devices, while majority states in the  $\text{NC}_4\text{N}$  device, corresponding to the behavior of spin-dependent transport in the two kinds of wires with or without intrinsic magnetism. Since there are total net magnetic moments in the isolated  $\text{NC}_3\text{N}$  and  $\text{C}_4$  wires, the number of occupied majority states must be more than that of minority states. It causes net majority states locating below the  $E_F$ , while minority states, above or around the  $E_F$ , giving rise to the minority conduct-

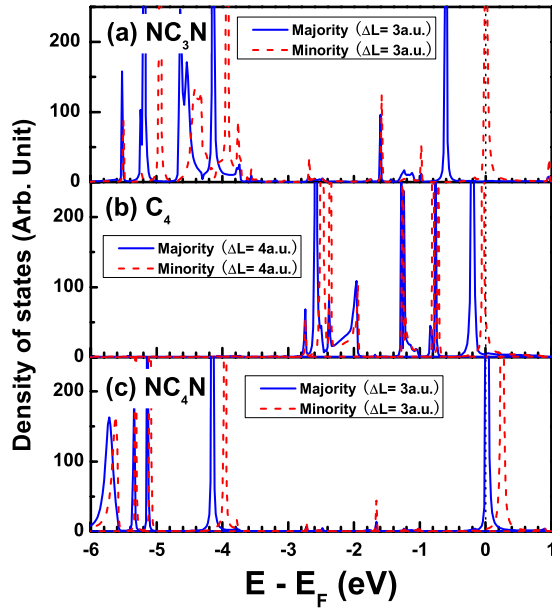


FIG. 4. (Color online) Density of states of the atomic wires  $\text{NC}_3\text{N}$ ,  $\text{C}_4$ , and  $\text{NC}_4\text{N}$  sandwiched between two gold electrodes. Note that the density of states from the buffer layers were subtracted.

ing channel in the devices. For  $\text{NC}_4\text{N}$ , no net majority states is required to lie below the  $E_F$ . After the wires are stretched, the majority states move down to  $E_F$ , leading to the majority states to be conducting.

Figure 5 shows the transmission coefficient as a function of the number of carbon atoms in the wires of  $\text{C}_n$  and  $\text{NC}_n\text{N}$  with the stretching of  $\Delta L=3$  a.u.. For comparison, results for  $\text{C}_n$  without stretching are also given [Fig. 5(a)]. No evident spin-polarized transport is found in  $\text{C}_n$  wires when  $\Delta L=0$  a.u., as discussed above. The total transmission coefficient in Fig. 5(a) shows an even-odd oscillatory behavior, consistent with previous result on carbon wires without consideration of magnetism.<sup>13,30</sup> When the  $\text{C}_n$  atomic wires are stretched with  $\Delta L=3$  a.u., only atomic wires with odd number of carbon atoms show clear spin-polarized transport. Larger stretching is usually needed to produce spin-polarized transport for  $\text{C}_n$  atomic wires with even number of carbon atoms, as seen in Fig. 3(c). The reason may be ascribed to strong C-C triple bonds near the ends of the wires in the case. The explicit even-odd oscillatory trend is also seen to happen for the total transmission coefficients in Fig. 5(b) even after the spin splitting occurs. This behavior keeps for the  $\text{NC}_n\text{N}$  wires with  $\Delta L=3$  a.u., shown in Fig. 5(c). This means spin-polarized transport does not destroy the even-odd oscillatory behavior of the total conductance in the wires. Perfect spin filtering effect can also be seen for all the wires of  $\text{NC}_n\text{N}$  from Fig. 5(c).

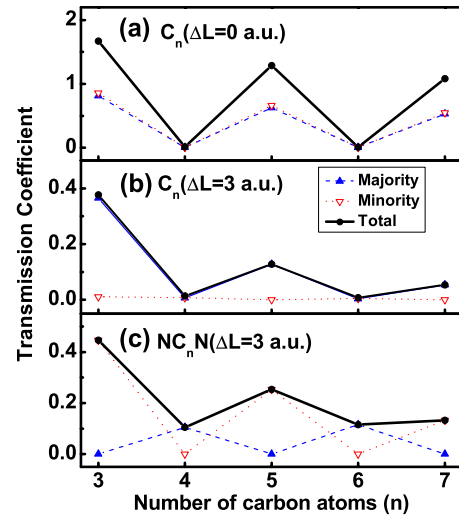


FIG. 5. (Color online) Transmission coefficient as a function of number of carbon atoms in (a)  $\text{C}_n$  wires without stretching, (b)  $\text{C}_n$  wires with  $\Delta L=3$  a.u., and (c)  $\text{NC}_n\text{N}$  wires with  $\Delta L=3$  a.u.. The majority and minority express the different spin directions. Their sum gives the total transmission coefficient.

In conclusion, we found that *isolated and short* carbon atomic wires may have very interesting magnetic properties, although the magnetism is significantly diminished when the wires are contacted by nonmagnetic metal leads. In particular, for  $\text{C}_{2n}$  atomic wires a total magnetic moment of  $2\mu_B$  was obtained. The magnetism is mostly localized at the terminals of the wires due to unpaired states. For nitrogen-doped wires,  $\text{NC}_{2n+1}\text{N}$  and  $\text{C}_n\text{NC}_n$ , the ground-state magnetic structure mimics a SDW-like state. No magnetism is found for the wires of  $\text{C}_{2n+1}$  and  $\text{NC}_{2n}\text{N}$ . The magnetic behaviors in the wires can be understood by the bonding patterns and the existence of unpaired states. Perfect spin filtering effect was obtained in the nitrogen-doped carbon wires sandwiched between Au leads by stretching the wires slightly. For the wires with or without intrinsic magnetism, different conducting mechanisms were found. The even-odd oscillatory behavior of the total conductance is seen for these atomic wires even after spin-polarized transport occurs in the systems. It is important to emphasize that the magnetism in these wires exists in finite-sized systems where spin coherence is not destroyed by thermal fluctuations. Our results suggest that carbon atomic wires may have very interesting applications in spin-polarized quantum transport in nanoelectronics.

#### ACKNOWLEDGMENTS

The work was supported by the National Natural Science Foundation of China under Grants No. 10674027 and No. 60771059, 973-project under grant No. 2006CB921300, and Fudan High-end Computing Center.



\*zyang@fudan.edu.cn

- <sup>1</sup>D. D. Awschalom and M. E. Flatte, *Nat. Phys.* **3**, 153 (2007); F. Kuemmeth, S. Ilani, D. C. Ralph, and P. L. McEuen, *Nature (London)* **452**, 448 (2008).
- <sup>2</sup>S. Sahoo, T. Kontos, J. Furer, C. Hoffmann, M. Gräber, A. Cottet, and C. Schönenberger, *Nat. Phys.* **1**, 99 (2005).
- <sup>3</sup>N. Tombros, S. J. van der Molen, and B. J. van Wees, *Phys. Rev. B* **73**, 233403 (2006).
- <sup>4</sup>J. A. Fürst, M. Brandbyge, A.-P. Jauho, and K. Stokbro, *Phys. Rev. B* **78**, 195405 (2008).
- <sup>5</sup>S. Dag, S. Tongay, T. Yildirim, E. Durgun, R. T. Senger, C. Y. Fong, and S. Ciraci, *Phys. Rev. B* **72**, 155444 (2005).
- <sup>6</sup>E. Durgun, R. T. Senger, H. Sevinçli, H. Mehrez, and S. Ciraci, *Phys. Rev. B* **74**, 235413 (2006).
- <sup>7</sup>C. K. Yang, *Appl. Phys. Lett.* **92**, 033103 (2008).
- <sup>8</sup>W. Harnett, *Phys. Rev. A* **65**, 032322 (2002).
- <sup>9</sup>M. Fujita, K. Wakabayashi, K. Nakada, and K. Kusakabe, *J. Phys. Soc. Jpn.* **65**, 1920 (1996).
- <sup>10</sup>Y. W. Son, M. L. Cohen, and S. G. Louie, *Nature (London)* **444**, 347 (2006).
- <sup>11</sup>J. J. Palacios, J. Fernandez-Rossier, and L. Brey, *Phys. Rev. B* **77**, 195428 (2008).
- <sup>12</sup>K. S. Novoselov, A. K. Geim, S. V. Morozov, D. Jiang, Y. Zhang, S. V. Dubonos, I. V. Grigorieva, and A. A. Firsov, *Science* **306**, 666 (2004).
- <sup>13</sup>N. D. Lang and Ph. Avouris, *Phys. Rev. Lett.* **81**, 3515 (1998).
- <sup>14</sup>B. Larade, J. Taylor, H. Mehrez, and H. Guo, *Phys. Rev. B* **64**, 075420 (2001).
- <sup>15</sup>S. Tongay, R. T. Senger, S. Dag, and S. Ciraci, *Phys. Rev. Lett.* **93**, 136404 (2004).
- <sup>16</sup>R. T. Senger, S. Tongay, S. Dag, E. Durgun, and S. Ciraci, *Phys. Rev. B* **71**, 235406 (2005).
- <sup>17</sup>P. Redondo, C. Barrientos, and A. Largo, *J. Phys. Chem. A* **109**, 8594 (2005); A. Largo, P. Redondo, and C. Barrientos, *ibid.* **108**, 6421 (2004).
- <sup>18</sup>R. Pati, M. Mailman, L. Senapati, P. M. Ajayan, S. D. Mahanti, and S. K. Nayak, *Phys. Rev. B* **68**, 014412 (2003).
- <sup>19</sup>Y. Wei, Y. Xu, J. Wang, and H. Guo, *Phys. Rev. B* **70**, 193406 (2004).
- <sup>20</sup>L. Senapati, R. Pati, M. Mailman, and S. K. Nayak, *Phys. Rev. B* **72**, 064416 (2005).
- <sup>21</sup>S. Eisler, A. D. Slepko, E. Elliott, T. Luu, R. McDonald, F. A. Hegmann, and R. R. Tykwinski, *J. Am. Chem. Soc.* **127**, 2666 (2005).
- <sup>22</sup>T. Ogata and Y. Tatamitani, *J. Phys. Chem. A* **112**, 10713 (2008).
- <sup>23</sup>G. Kresse and J. Furthmüller, *Phys. Rev. B* **54**, 11169 (1996); G. Kresse and J. Hafner, *ibid.* **49**, 14251 (1994).
- <sup>24</sup>G. Kresse and D. Joubert, *Phys. Rev. B* **59**, 1758 (1999); P. E. Blöchl, *ibid.* **50**, 17953 (1994).
- <sup>25</sup>J. Taylor, H. Guo, and J. Wang, *Phys. Rev. B* **63**, 245407 (2001); **63**, 121104(R) (2001).
- <sup>26</sup>G. Q. Li, J. Cai, J. K. Deng, A. R. Rocha, and S. Sanvito, *Appl. Phys. Lett.* **92**, 163104 (2008).
- <sup>27</sup>Y. J. Lee, M. Brandbyge, M. J. Puska, J. Taylor, K. Stokbro, and R. M. Nieminen, *Phys. Rev. B* **69**, 125409 (2004).
- <sup>28</sup>F. Chen, X. Li, J. Hihath, Z. Huang, and N. Tao, *J. Am. Chem. Soc.* **128**, 15874 (2006); A. I. Yanson, G. R. Bollinger, H. E. van den Brom, N. Agrait, and J. M. van Ruitenbeek, *Nature (London)* **395**, 783 (1998).
- <sup>29</sup>D. Waldron, P. Haney, B. Larade, A. MacDonald, and H. Guo, *Phys. Rev. Lett.* **96**, 166804 (2006); R. Liu, S. H. Ke, W. Yang, and H. U. Baranger, *J. Chem. Phys.* **127**, 141104 (2007).
- <sup>30</sup>Due to different models adopted for the electrodes, our obtained values of the transmission coefficients are somewhat different from those reported in Ref. 13. In particular, we used atomic electrodes with full band structure while Ref. 13 used jellium electrodes having one parabola band. Nevertheless, the even-odd oscillatory behavior was qualitatively the same.